

GigaScience

Construction and visualization of annotated pangenome networks enable graphical analyses for prokaryotic genetic diversity

--Manuscript Draft--

Manuscript Number:	GIGA-D-18-00147	
Full Title:	Construction and visualization of annotated pangenome networks enable graphical analyses for prokaryotic genetic diversity	
Article Type:	Research	
Funding Information:	National Natural Science Foundation of China (31601073)	Dr Junhua Li
Abstract:	<p>Pangenome analyses facilitate the interpretation of genetic diversity and evolutionary history of a taxon. However, there is an urgent and unmet need to develop new tools for advanced pangenome construction and visualization, especially for metagenomic data. Here we present an integrated pipeline, named MetaPGN, for graphically construction and visualization of pangenome networks from microbial genomes or metagenomes. Given isolate genomes or metagenomic assemblies coupled with a reference genome of the targeted taxon, MetaPGN generates a pangenome in a topological network, consisting of genes (nodes) and gene-gene genomic adjacencies (edges) of which biological information can be easily updated and retrieved. MetaPGN also includes a self-developed Cytoscape plugin for layout of and interaction with the resulting pangenome network, providing an intuitive and interactive interface for fully exploration of genetic diversity. We demonstrate the utility of MetaPGN by constructing Escherichia coli (E. coli) pangenome networks from five E. coli pathogenic strains and 760 human gut microbiomes respectively, revealing extensive genetic diversity of E. coli within both isolates and gut microbial populations. With the ability to extract and visualize gene contents and gene-gene physical adjacencies of a specific taxon from large-scale metagenomic data, MetaPGN provides advantages in expanding pangenome analysis to uncultured microbial taxa. MetaPGN is available at https://github.com/peng-ye/MetaPGN.</p>	
Corresponding Author:	Junhua Li, Ph.D. BGI shenzhen, guangdong CHINA	
Corresponding Author Secondary Information:		
Corresponding Author's Institution:	BGI	
Corresponding Author's Secondary Institution:		
First Author:	Ye Peng	
First Author Secondary Information:		
Order of Authors:	Ye Peng	
	Shanmei Tang	
	Dan Wang	
	Huanzi Zhong	
	Huijue Jia	
	Xianghang Cai	
	Zhaoxi Zhang	
	Minfeng Xiao	
	Huanming Yang	

	Jian Wang
	Xun Xu
	Junhua Li, Ph.D.
Order of Authors Secondary Information:	
Additional Information:	
Question	Response
Are you submitting this manuscript to a special series or article collection?	No
<p>Experimental design and statistics</p> <p>Full details of the experimental design and statistical methods used should be given in the Methods section, as detailed in our Minimum Standards Reporting Checklist. Information essential to interpreting the data presented should be made available in the figure legends.</p> <p>Have you included all the information requested in your manuscript?</p>	Yes
<p>Resources</p> <p>A description of all resources used, including antibodies, cell lines, animals and software tools, with enough information to allow them to be uniquely identified, should be included in the Methods section. Authors are strongly encouraged to cite Research Resource Identifiers (RRIDs) for antibodies, model organisms and tools, where possible.</p> <p>Have you included the information requested as detailed in our Minimum Standards Reporting Checklist?</p>	Yes
<p>Availability of data and materials</p> <p>All datasets and code on which the conclusions of the paper rely must be either included in your submission or deposited in publicly available repositories (where available and ethically appropriate), referencing such data using a unique identifier in the references and in the “Availability of Data and Materials” section of your manuscript.</p> <p>Have you have met the above requirement as detailed in our Minimum</p>	No

Standards Reporting Checklist?	
<p>If not, please give reasons for any omissions below.</p> <p>as follow-up to "Availability of data and materials</p> <p>All datasets and code on which the conclusions of the paper rely must be either included in your submission or deposited in publicly available repositories (where available and ethically appropriate), referencing such data using a unique identifier in the references and in the "Availability of Data and Materials" section of your manuscript.</p> <p>Have you have met the above requirement as detailed in our Minimum Standards Reporting Checklist?</p> <p>"</p>	<p>We are uploading assembled contigs of 760 metagenomes used in this study to EBI and CNSA, and will provide accession numbers when it is done.</p>

Construction and visualization of annotated pangenome networks enable graphical analyses for prokaryotic genetic diversity

Abstract

Pangenome analyses facilitate the interpretation of genetic diversity and evolutionary history of a taxon. However, there is an urgent and unmet need to develop new tools for advanced pangenome construction and visualization, especially for metagenomic data. Here we present an integrated pipeline, named MetaPGN, for graphically construction and visualization of pangenome networks from microbial genomes or metagenomes. Given isolate genomes or metagenomic assemblies coupled with a reference genome of the targeted taxon, MetaPGN generates a pangenome in a topological network, consisting of genes (nodes) and gene-gene genomic adjacencies (edges) of which biological information can be easily updated and retrieved. MetaPGN also includes a self-developed Cytoscape plugin for layout of and interaction with the resulting pangenome network, providing an intuitive and interactive interface for fully exploration of genetic diversity. We demonstrate the utility of MetaPGN by constructing *Escherichia coli* (*E. coli*) pangenome networks from five *E. coli* pathogenic strains and 760 human gut microbiomes respectively, revealing extensive genetic diversity of *E. coli* within both isolates and gut microbial populations. With the ability to extract and visualize gene contents and gene-gene physical adjacencies of a specific taxon from large-scale metagenomic data, MetaPGN provides advantages in expanding pangenome analysis to uncultured microbial taxa. MetaPGN is available at <https://github.com/peng-ye/MetaPGN>.

Keywords: pangenome, visualization, metagenomics

Introduction

The concept of pangenome, defined as the full complement of genes in a clade, was first introduced by Tettelin *et al.* in 2005 [1]. Pangenome analyses of a species now provide insights into core- and accessory-genome profiles, within-species genetic diversity, evolutionary dynamics and niche-specific adaptations. Hitherto, plenty of tools have been proposed for pangenome analysis on genomic or metagenomic data (Table 1).

Typical pangenome tools such as GET_HOMOLOGUES [2] and PGAP [3], mainly focus on analyzing the homologous gene families and calculating the core/accessory genes of a given taxon. However, these tools cannot provide the variations of gene-gene physical relationships. Tools like GenoSets [4], PGAT [5], PEGR [6], EDGAR [7], GenomeRing [8] and PanViz [9] are developed to generate a linear or circular presentation of homologous sequences/genes, which can indicate the physical relationships between genomic sequences or genes. However, these tools visualize the core/accessory sequences or genes on independent lines and thus cannot intuitively present the complex variations among the input genomes.

Pangenomes built using *de Bruijn* graph, like SplitMEM [10] and a tool introduced by Baier *et al.* [11], partly solve the above problems. In the resulting graph yielded by these tools, complete pan-genome is represented in a compact graphical representation such that the core/accessory status of any genomic sequences is immediately identifiable, along with the context of the flanking sequences. This strategy enables powerful topological analysis of the pan-genome not possible from a linear/circular representation. Nevertheless, tools based on the *de Bruijn* graph algorithm can only construct a compact network comprised of core/accessory genomic sequences instead of genes, which means retrieving or updating functional information in downstream analysis will be difficult. Furthermore, these tools do not visualize the constructed *de Bruijn* graph and provide an interactive interface for users to explore the graph.

Moreover, all the above-mentioned tools analyzed pangenomes via genomic data which require organisms isolated from the environment and cultured *in vitro*. Recent advances in metagenomics have led to a paradigm shift in pangenome study from a limited quantity of cultured microbial genomes to large-scale metagenomic datasets containing huge potential of functional and phylogenetic resolution from the nonculturable taxa. Several existing tools dealing with

1
2
3
4 metagenomic data are based on constructed pangenomes, namely; cannot utilize the abundant gene
5 resources contained in metagenomes to extend the pangenomes in question. For example,
6 PanPhlAn [12], MIDAS [13], and a pipeline introduced by Delmont and Eren [14] map reads onto
7 a reference pangenome, to describe the pattern of presence/absence of genes in metagenomes. For
8 another instance, Kim *et al.* [15] clustered genes predicted from metagenomic contigs with
9 Bacillus core genes for profiling the Bacillus species in the microbiomes. Recently, Farag *et al.*
10 [16] aligned metagenome contigs with reference genomes for identification of “*Latescibacteria*”
11 genomic fragments. Though this strategy can theoretically recruit sequences not present in the
12 reference genomes, it is likely to filter out “*Latescibacteria*” genomic fragments with structural
13 variations compared to the reference ones. Furthermore, all these aforementioned methods for
14 metagenomic data did not organize the pangenome using a network, which is essential for
15 efficiently storage and visualization of pangenome constructed from metagenomic data.
16
17
18
19
20
21
22
23
24
25

26
27 Here, we introduce an integrated pipeline (MetaPGN) for network-based construction and
28 visualization of prokaryotic pangenomes for both bacterial genomes and metagenomes. Given
29 genomic or metagenomic assemblies and a reference genome of a taxon of interest, MetaPGN
30 derives a pangenome network for integrating genes (nodes) and gene-gene adjacencies (edges)
31 belonging to this taxon. MetaPGN also includes a specific Cytoscape plugin for layout of and
32 interaction with the resulting pangenome network, providing an intuitive and interactive interface
33 for the exploration of gene diversity. For example, in the visualized network in Cytoscape, users
34 can specify gene annotations, customize the appearance of nodes and edges, search and concentrate
35 on genes of certain functions. We applied MetaPGN on assemblies from five pathogenic *E. coli*
36 strains and 760 human gut microbiomes respectively, with *E. coli* K-12 substr. MG1655 (*E. coli* K-
37 12) being the reference genome. It showed that by taking gene adjacency into account and
38 visualizing the pangenome network in a well-organized manner, MetaPGN can assist in observing
39 genetic diversity in genomic or metagenomic assemblies graphically and conveniently.
40
41
42
43
44
45
46
47
48
49
50
51
52
53
54
55
56
57
58
59
60
61
62
63
64
65

Results

General workflow. MetaPGN accepts genome or metagenome assemblies as input (query assemblies) and requires a reference genome for recruitment of the query assemblies and as the skeleton of the pangenome network. The MetaPGN pipeline can be divided into two main parts: (i) construction of a pangenome network comprised of representative genes, including gene prediction, gene redundancy elimination, gene type determination, pairwise gene adjacency extraction, assembly recruitment (for metagenomic assemblies) and pangenome network generation and, (ii) visualization of the pangenome network in an organized way, where nodes represent genes and edges indicate gene adjacencies, in Cytoscape [17] with a self-developed plugin (Fig. 1, Fig. S1, and Methods). From the resultant pangenome network, the degree of similarity among homologous genes, as well as their genomic context is easily visible. Also of note is that users can add and update annotation for nodes and edges in the networks, based on which elements of interest can be accessed conveniently.

Pangenome network of 5 pathogenic *Escherichia coli* genomes. In order to demonstrate its potential in studying microbial genetic diversity and phenotype-genotype relationship, we first applied MetaPGN on genomes of 5 pathogenic *E. coli* isolates, *E. coli* O26:H11 str. 11368, *E. coli* O127:H6 E2348/69, *E. coli* O157:H7 str. EDL933, *E. coli* O104:H4 str. 2011C-3493 and *E. coli* 55989. A commensal *E. coli* strain, K-12 substr. MG1655 (Supplementary Table S1) was chosen as the reference genome in this instance and in all examples shown below.

A pangenome network consisting of 9,161 nodes and 11,788 edges (Supplementary Table S3, Supplementary File 2) was constructed and visualized (Methods). Based on the well visualized pangenome network along with functional annotation, we can now graphically observe the extent of variations of certain genes, as well as their genomic context. For example, when focusing on a cluster of flagellar genes (Fig. 2a), we found that *fliC* genes coding the filament structural protein (H-antigen) and *fliD* gene coding the filament capping protein are highly variable among these *E. coli* strains. In contrast, four genes coding chaperones (*fliS*, *fliT*, *fliY*, *fliZ*) and a gene (*fliA*) relating to the regulation of the expression of flagellar components are conserved over all the *E. coli* strains investigated. A gene (270 bp) coding hypothetical protein is uniquely presented between *fliC* and *fliD* in *E. coli* O157:H7 str. EDL933.

1
2
3
4 In a fimbria protein-related gene cluster, compared to the reference *E. coli* strain, all the 5
6 pathogenic strains possess several genes located between two conserved genes coding an outer
7 membrane protein and a regulatory protein, and *E. coli* O127:H6 E2348/69 uniquely exhibits more
8 genes encoding proteins of unknown functions (Fig. 2b).
9

10
11 For a gene cluster responsible for the biosynthesis of lipopolysaccharides, *E. coli* O127:H6
12 E2348/69 shares three genes with reference strain, that differentiate from the other 4 pathogenic
13 strains (Fig. 2c). For another gene cluster of related function, the *E. coli* O127:H6 E2348/69 also
14 shows a strain-specific duplication event of two colonic acid (CA)-related genes (*wcaH* and *wcaG*,
15 denoted by a purple dash line in Fig. 2d). It has been demonstrated that CA can modify
16 lipopolysaccharide (LPS) into a novel form (M_{LPS}) which may enhance survival of *E. coli* in
17 different putative ways [18]. The two *wcaH* genes in *E. coli* O127:H6 E2348/69, though share
18 high similarity (99.1% identity), may confer the strain with diverse functional potentials for CA
19 formation and thereby the novel survival mechanism yet unknown.
20

21 In addition, the German outbreak *E. coli* O104:H4 str. 2011C-3493 comprises identical nodes and
22 edges in the flagellar-related gene cluster (Fig. 2a) and the O antigen-related gene cluster with a
23 historical *E. coli* 55989 (Fig. 2d), suggesting the close
24 evolutionary relationship between these strains as previously reported [19,20].
25

26 These results demonstrate the feasibility of MetaPGN for construction and visualization of
27 microbial pangenomes in an organized way. Moreover, by involving genomic adjacency and
28 offering easy-to-achieve biological information, MetaPGN provides a convenient way to assist
29 biologists in exposing genetic diversity for genes of interest among the organisms under study.
30

31
32
33
34
35 **Pangenome network of *E. coli* in 760 metagenomes.** Moving beyond surveying the pangenome
36 network of isolate genomes, we applied MetaPGN in metagenomic datasets to interrogate the *E.*
37 *coli* pangenome network on a grander scale. Assemblies of 760 metagenomes sequenced in the
38 Metagenomics of the Human Intestinal Tract (MetaHIT) project [21–24] were collected, which
39 contained 8,096,991 non-redundant genes with annotations [24]. As metagenome assemblies are
40 from varied taxa, it is necessary to recruit assemblies of the targeted taxon before construction of
41 the pangenome network. In this study, metagenome assemblies were recruited using a gene
42 alignment-based strategy, which was assessed with mock datasets (Methods). With the recruited
43
44
45
46
47
48
49
50
51
52
53
54
55
56
57
58
59
60
61
62
63
64
65

1
2
3
4 assemblies, a pangenome network consisting of 9,406 nodes and 14,676 edges (Supplementary
5 Table S3, Supplementary File S3) was generated and visualized after refinement (Methods).

6
7
8 Based on annotation, we first searched flagellin-related genes in this network. We found that
9 the pattern of adjacencies among these genes was similar to that in the pangenome network of the
10 5 pathogenic *E. coli* genomes: *fliC* and *fliD* are hypervariable while *fliT*, *fliY*, *fliZ* and *fliA* are very
11 conserved among these 760 samples. However, some genes of unknown function locate between
12 *fliC* and *fliA* (Fig. 3a), instead of between *fliC* and *fliD* in the pangenome network of the 5
13 pathogenic *E. coli* strains (Fig 2a).

14
15
16 We then investigated mobile genetic elements (MGEs) in this pangenome network, as they can
17 induce various types of genomic rearrangements[25]. Of the 362 nodes (~4%) annotated as MGE-
18 related (according to Cluster of Orthologous Groups annotation done in reference 28), many were
19 flanked by different shared genes on different *E. coli* genomes. In a region of the network, a gene
20 cluster containing MGEs is query-specific, indicating there might be genomic rearrangements
21 caused by strain-specific MGEs within the *E. coli* species (Fig. 3b). In another part of the network
22 harboring MGEs, we observed that several branches of non-MGE genes are inserted in between
23 two MGEs, which may imply a mutation hotspot within the region, or the existence of MGEs as
24 yet undescribed (Fig. S1).

25
26
27 Application of MetaPGN in large-scale metagenomic data generated an *E. coli* pangenome
28 network that might hardly be constructed from isolated genomes. As demonstrated here, the
29 assembly-recruitment based, well-organized and visualized pangenome network can greatly
30 expand our understanding in the genetic diversity of a taxon, although further efforts in
31 bioinformatic and experimental analyses are needed to verify and extend these findings.

32
33
34
35
36
37
38
39
40
41
42
43
44
45
46
47
48 **Assessment of pangenome networks derived from metagenomes.** Genomic sequences
49 assembled from metagenomic data are usually fragmentary resulted from limitations in sequencing
50 platforms and bioinformatic algorithms. Due to this nature, a pangenome network recovered from
51 a limited number of assemblies is likely to be segmented compared to a complete genome. To
52 propose a minimum size of assemblies for getting a relatively connected pangenome network, we
53 assessed the completeness of *E. coli* pangenome networks derived from varying size of recruited
54 assemblies (Methods). As shown in Fig. 4, the count of connected subnetworks drops dramatically
55
56
57
58
59
60
61
62
63
64
65

1
2
3
4 with the total length of recruited assemblies increasing from 5 Mb to 50 Mb (roughly from 1 × to
5
6 10 × of a *E. coli* genome), then barely changes even when using all recruited assemblies of the
7
8 dataset (215 Mb, from 760 samples). Based on this analysis, a minimum size of recruited
9
10 assemblies 10-fold of the studied genome is required to generate a relatively intact pangenome
11
12 network when constructed from metagenomes.
13

14 15 Discussion

16
17
18 Since first coined more than a decade ago, pangenome analysis has provided a framework for
19
20 studying the genomic diversity within a species. Current methods for pangenome analyses mainly
21
22 focus on gene contents but ignore their genomic context, as well as have shortages in pangenome
23
24 visualization. Besides, available methods are usually designed for genomic data and not capable
25
26 of constructing pangenomes from metagenomics data. To fill these gaps, our MetaPGN pipeline
27
28 takes genome or metagenome assemblies as input, uses gene contents as well as pairwise gene
29
30 adjacency to generate a compact graphical representation for the gene network based on a reference
31
32 genome, and visualizes the network in Cytoscape with a self-developed plugin (Fig. 1, Fig. S2).
33

34 From the two MetaPGN-derived *E. coli* pangenome networks, we can directly observe the
35
36 diversity of genes among the five pathogenic *E. coli* strains and 760 human gut microbiomes with
37
38 respect to the reference genome. For instance, in the pangenome network for the 5 pathogenic *E.*
39
40 *coli* strains, we found that gene *fliC* which carries H-antigen specificity were highly variable
41
42 among the *E. coli* assemblies (Fig. 2a). This *fliC* gene was more varied in the 760 human gut
43
44 microbiomes (Fig. 3a). In addition, genes for synthesis of O-antigen and outer membrane protein
45
46 showed a great diversity in the pangenome network of the 5 *E. coli* strains (Fig. 2c, Fig. 2d). These
47
48 results are in agreement with previous findings on H-antigen specificity related genes [26–28] and
49
50 O-antigen related genes [29,30]. We also showed that when gene adjacency is incorporated into
51
52 the construction and visualization of pangenomes, locations of genes of unknown function are
53
54 identified, which may be helpful for the inference of their biological functions. For example, in
55
56 both the two pangenome networks, we found genes of unknown function locating between the *fliC*
57
58 gene and other flagellin-related genes (Fig. 2a, located between *fliC* and *fliD*, Fig. 3a, located
59
60 between *fliC* and *fliA*), indicating that these function-unknown genes may play a role in flagellin
61
62 biosynthesis [31], although further experimental trials are needed to prove this point. Additionally,
63
64
65

1
2
3
4 from the pangenome network of the five *E. coli* strains, we observed a great variation event on *E.*
5 *coli* O127:H6 E2348/69, which was further verified to stem from a duplication event of two
6 colonic acid (CA)-related genes (*wcaH* and *wcaG*, Fig 2d). This finding indicates that knowledge
7 of genomic adjacency may also shed light on further studying structural variations among the input
8 assemblies. If extended, genomic adjacency may help in finding possible functional sequences
9 which potentially drive variations such as genomic repeats discussed by Delihis [32] and Wang *et*
10 *al.* [33], and lead to the discovery of new functional modules as illustrated by Doron *et al.* [34].
11 These examples show that visualizing a pangenome involving gene adjacencies, and providing
12 easy-to-add and retrieve biological information, is of significance.
13
14
15
16
17
18
19
20

21 Although examples shown in this study use the genome of a commensal *E. coli* strain for
22 assembly recruitment and network arrangement, users can specify the reference genome when
23 applying MetaPGN. Epidemiologists can use MetaPGN to compare assemblies of outbreak strains
24 or viruses, such as *Vibrio cholerae* or Ebola virus, with those of some well-studied pathogenic
25 strains to find novel variations involved in pathogenesis, which may further provide candidate
26 targets for drug and vaccine design [35,36]. Moreover, pangenome networks built from
27 metagenomes of different cohorts may help us better observe and compare the diversity of a
28 species among these cohorts, and may thus give a hint to explain the inconsistent findings of certain
29 disease-related gut microbes. For instance, Fredrik *et al.* reported that *Prevotella copri* (*P. copri*)
30 improved hosts' glucose metabolism [37] while Oluf *et al.* argued that *P. copri* induced insulin
31 resistance [38]. MetaPGN can therefore be used to build a pangenome network of these disease-
32 related microbes, and study the genetic variations which might explain these inconsistent findings.
33
34
35
36
37
38
39
40
41
42
43

44 It should be noticed that, in this pipeline, we compare genes depending on nucleotide-level
45 sequence identity and overlap: genes with $\geq 95\%$ identity and $\geq 90\%$ overlap are regarded as the
46 same gene. However, as we know, genes of the same function may not satisfy this criterion ($\geq 95\%$
47 identity and $\geq 90\%$ overlap), whereas protein encoded by these genes can be less diverse. Hence,
48 in our future work, we can cluster genes by comparing their nucleotide sequences as well as the
49 amino acid sequences. Besides, the current MetaPGN pipeline does not consider other genomic
50 features, nor physical distances between genes in constructing the pangenome network. However,
51 differences in other genomic features such as ribosomal binding site (RBS) sequences [39,40] and
52 distances between the RBS and start codons [41] may result in distinct phenotypes. Therefore,
53 users can involve these information in analyzing pangenome networks as well.
54
55
56
57
58
59
60
61
62
63
64
65

1
2
3
4 To conclude, MetaPGN would serve to directly observe genetic diversity in pangenome
5 networks, better understand genotype-phenotype relationships and the evolutionary history.
6
7
8
9

10 Methods

11
12 **Pangenome network construction in MetaPGN.** First, gene prediction of query assemblies is
13 performed using MetaGeneMark (Version 2.8) [42]. In order to eliminate redundancy, the resultant
14 genes are clustered by CD-HIT (Version 4.5.7) [43] with identity $\geq 95\%$ and overlap $\geq 90\%$, and
15 genes in a same cluster are represented by the longest sequence of the cluster which is called the
16 representative gene. Representative genes of all clusters are subsequently aligned against genes on
17 the given reference genome using BLAT (Version 34) [44]. From the alignment result, genes
18 shared between the representative gene set and the reference gene set with identity $\geq 95\%$
19 and overlap $\geq 90\%$ are defined as ‘shared genes’. The remaining representative and reference genes
20 other than those shared genes are defined as ‘query-specific genes’ and ‘reference-specific genes’,
21 respectively. Pairwise gene physical adjacency of representative genes on the query assemblies
22 and of reference genes are then extracted, and status for each adjacency of being ‘shared’, ‘query-
23 specific’, or ‘reference-specific’ is determined. Finally, based on the recruited assemblies and the
24 reference genome, an initial pangenome network is generated: each node stands for a reference
25 gene or a representative gene on the recruited assemblies; two nodes are connected by an edge if
26 they are physically adjacent on the recruited assemblies or on the reference genome. The weight
27 of a node or an edge denotes its occurrence frequency on all of the recruited assemblies and the
28 reference genome.
29
30
31
32
33
34
35
36
37
38
39
40
41
42
43
44

45
46 **Pangenome network visualization in MetaPGN.** The following preprocessing work on the
47 initial pangenome network was implemented before visualization: 1. The initial pangenome
48 network was refined by removing isolated networks (networks not connected with the backbone)
49 and tips (nodes only connected with another node); 2. Nodes and edges were added with some
50 extra attributes, such as the status of the nodes and edges (query-specific, reference-specific or
51 shared), whether the genes for the nodes were phage-, plasmid-, CRISPR- related genes and so on
52 (**Supplementary Table S3**). Users can specify the attributes of nodes and edges according to their
53 own datasets.
54
55
56
57
58
59
60
61
62
63
64
65

1
2
3
4 We then used a self-developed Cytoscape plugin to visualize the pangenome network in an
5 organized way (Supplementary Text 1 in Supplementary File S1 illustrates how to install the
6 plugin in Cytoscape). Our algorithm for organizing nodes in the network is as follows:
7
8
9

- 10 1. Construct a circular skeleton for the pangenome network with shared nodes and reference-
11 specific nodes, according to positions of their related reference genes on the reference genome.
12 If there are two or more representative genes similar to the same reference gene ($\geq 95\%$ identity
13 and $\geq 90\%$ overlap), use one of these representative genes to construct the skeleton and place
14 the others on both sides of the skeleton in turn (Fig. S2 a).
15
16
17
18
19 2. Arrange query-specific nodes region by region, including,
20
21 2.1. Select query-specific nodes in a region spanning less than 30 nodes in the skeleton
22 (see Supplementary Text 2 in Supplementary File S1 for more details).
23
24 2.2. Arrange these query-specific nodes as follows,
25
26 i. For those that directly link with two nodes on the skeleton, place them on the bisector
27 of the two skeleton nodes. If there are two or more query-specific nodes directly
28 linking with the same pair of nodes on the skeleton, place them on both sides of the
29 bisector of these pair of skeleton nodes in turn (Fig. S2 b).
30
31
32
33 ii. Among the remaining nodes, for those that directly link with two placed nodes, place
34 them on the bisectors of the placed ones. Iterate this step for five times (Fig. S2 c).
35
36
37
38 iii. For the remaining nodes, place them into an arc without moving the placed nodes (Fig.
39 S2 d), or else place them one by one starting near a placed node (Fig. S2 e).
40
41
42
43

44 **Construction and visualization of the 5-*E. coli*-genome pangenome network.** Genes were
45 extracted from the reference genome for each strain (Supplementary Table S1). Using *E. coli* K-
46 12 as the reference, a pangenome network was generated following Step 2-6 described above. In
47 the visualization of this pangenome network, we used green, blue and red color to denote a
48 reference-specific, shared, and query-specific node or edge, respectively, and specified sizes of
49 nodes and widths of edges with their occurrence frequency in the input genomes.
50
51
52
53
54
55
56

57 **Assessment of the gene alignment-based assembly recruitment strategy.** A gene alignment-
58 based strategy was used for recruitment of metagenome assemblies in this study, which considers
59
60
61
62
63
64
65

1
2
3
4 1) the count of genes on an assembly (c), and 2) the ratio of the number of shared genes (designated
5 as aforementioned) on an assembly to the total number of genes on that assembly (r). $c = 3$ paired
6 with $r = 0.5$, requiring at least 3 genes including 2 shared genes containing in an assembly, was
7 chosen for recruitment of metagenome assemblies in this study.
8
9

10
11
12 5 mock metagenomic datasets were used to assess the performance of this strategy. Briefly,
13 simulated reads of 50 bacterial genomes from 10 common genera present in the human gut were
14 generated by iMESSi [45], including the 5 pathogenic *E. coli* strains mentioned above
15 (Supplementary Table S1). Each dataset was simulated at the same complexity level with 80
16 million (M) 80bp paired-end reads of 10 strains from 10 different genera and the relative
17 abundances of strains were assigned by the broken-stick model (Supplementary Table S2).
18 Simulated reads were first independently assembled into assemblies by SOAPdenovo2 in each
19 dataset [43], with an empirical k-mer size of 41. Genes were then predicted on assemblies longer
20 than 500 bp using MetaGeneMark [40] (default parameters were used except the minimum length
21 of genes was set as 100 bp).
22
23
24
25
26
27
28
29
30

31 Assemblies of each mock dataset were first aligned against the 5 pathogenic *E. coli* reference
32 genomes by BLAT[44]. Those assemblies that have an overall $\geq 90\%$ overlap and $\geq 95\%$ identity
33 with the reference genomes were considered as *E. coli* genome-derived (traditional genome
34 alignment-based strategy) and were recruited for construction of a reference pangenome network
35 (RPGN). A query pangenome network (QPGN) was then generated from assemblies selected by
36 the gene alignment-based strategy with $c = 3$ and $r = 0.5$ as described above.
37
38
39
40
41
42

43 Accuracy of query assembly recruitment was assessed, in respect of conformity and divergence
44 between the RPGN with the QPGN (Supplementary Text 3 and 4 in Supplementary File S1). The
45 result showed that the QPGN recovered 87.9% of node and 90.3% of edge in the RPGN, while
46 falsely included 0% of node and less than 1% of edge, which demonstrated the high accuracy of
47 the gene alignment-based strategy for recruitment of metagenome assemblies.
48
49
50
51
52
53

54 **Construction and visualization of the 760-metagenome pangenome network.** Assemblies and
55 representative genes of the 760 metagenomes generated in Reference [24] were used here, since
56 they were produced using identical methods and parameter settings in this study. A pangenome
57 network was generated following steps described above, again using *E. coli* K-12 as the reference,
58
59
60
61
62
63
64
65

1
2
3
4 and $c = 3$, $r = 0.5$ for assembly recruitment. The resulting pangenome network was visualized in
5
6 the same way as visualizing the 5-*E. coli*-genome pangenome network.
7
8
9

10 **Analysis of subnetworks comprising a pangenome network.** 10-700 metagenomes were
11 randomly sampled from the above-mentioned 760 metagenomes. For each sub-dataset, a
12 pangenome network was constructed after assembly recruitment using *E. coli* K-12 as the
13 reference genome. For each pangenome network, reference-specific edges were removed before
14 counting the number of subnetworks. Only sub-datasets with a size of recruited assemblies greater
15 than 5 Mb were used to generate the scatterplot, in which a curve with 95% confidential intervals
16 was fitted by the ‘loess’ smoothing method in R [46].
17
18
19
20
21
22
23
24
25

26 **Data availability.** Genome sequence of 50 strains (contained 5 *E. coli* genomes) and the reference
27 genome were downloaded from the National Center for Biotechnology Information
28 (<ftp://ftp.ncbi.nlm.nih.gov/genomes/refseq/bacteria/>). Please refer to **Supplementary Table S1** for
29 detailed information. Raw sequences of the 5 mock metagenomics datasets are available in the
30 EBI repository [/to/be/uploaded](#). The MetaPGN pipeline, and Cytoscape session files for *E. coli*
31 pangenome networks derived from five pathogenic *E. coli* strains and from 760 metagenomes are
32 available on Github (<https://github.com/peng-ye/MetaPGN>).
33
34
35
36
37
38
39
40
41

42 List of Figures

43
44

45 **Figure 1.** An Overview of the MetaPGN pipeline: from assemblies to a pangenome network. Gene
46 prediction is performed on query assemblies. The resulting genes are clustered, after which genes
47 in the same cluster are represented by the longest sequence of this cluster called the representative
48 gene (node a-g). All these representative genes are then aligned against genes on the given
49 reference genome. From the alignment result, genes shared between the representative gene set
50 and the reference gene set are defined as ‘shared’ genes (blue). The remaining representative and
51 reference genes other than those shared genes are defined as ‘query-specific’ genes (red) and
52 ‘reference-specific’ genes (green), respectively. Pairwise gene physical adjacency of
53
54
55
56
57
58
59
60
61
62
63
64
65

1
2
3
4 representative genes on the query assemblies and of reference genes are then extracted, and status
5 for each adjacency of being ‘shared’ (blue), ‘query-specific’ (red), or ‘reference-specific’ (green)
6 is determined. Finally, based on the recruited assemblies and the reference genome, a pangenome
7 network is generated: each node stands for a reference gene or a representative gene on the
8 recruited assemblies; two nodes are connected by an edge if they are physically adjacent on the
9 recruited assemblies or the reference genome. The weight of a node or an edge is its occurrence
10 frequency on all of the recruited assemblies and the reference genome (Methods). The pangenome
11 network is then visualized in Cytoscape with a self-developed plugin (Methods) for a better
12 arrangement. Biological information of nodes and edges, such as gene name and annotation, can
13 be easily retrieved in the interactive user interface in Cytoscape.
14
15
16
17
18
19
20
21
22

23 **Figure 2.** Subgraphs of highly variable genes in the pangenome network of 5 pathogenic *E. coli*
24 strains (manually arranged). (a) a cluster of flagellar genes. (b) a cluster containing outer
25 membrane protein-coding genes. (c) a cluster of genes responsible for biosynthesis of the O antigen.
26 (d) another cluster of O antigen-related genes. Green, blue, red nodes and edges denote reference-
27 specific, shared, and query- specific genes and gene adjacencies, respectively. Size of nodes and
28 thickness of edges indicates their weight (occurrence frequency). Numbers alongside shared genes
29 are their indexes in the representative gene set.
30
31
32
33
34
35

36 **Figure 3.** Two subgraphs of the pangenome network of *E. coli* constructed from 760 metagenomes
37 (manually arranged). (a) a cluster of flagellar genes. (b) a cluster of genes containing MGEs. Green,
38 blue, red nodes and edges denote reference-specific, shared, and query- specific genes and gene
39 adjacencies. Triangles represent MGEs. Size of nodes and thickness of edges indicates their weight
40 (occurrence frequency). Numbers alongside shared genes are their indexes in the representative
41 gene set.
42
43
44
45
46

47 **Figure 4.** Number of subnetworks in pangenome networks derived from varying sizes of recruited
48 assemblies. The x-axis indicates total length of recruited assemblies for each sub-dataset and the
49 y-axis represents the number of subnetworks in the pangenome network derived from each sub-
50 dataset. The curve was fitted for the scatters using the ‘loess’ smoothing method in R[46]. The
51 shaded area displays the 95% confidential intervals of the curve. Axes are log₂-transformed.
52
53
54
55
56
57
58

59 Additional information 60 61 62 63 64 65

1
2
3
4 **Supplementary Figure S1.** Another cluster of genes containing MGEs, flanked by different shared
5 genes on different *E.coli* genomes (manually arranged). Green, blue, red nodes and edges denote
6 reference-specific, shared, and query- specific genes and gene adjacencies. Triangles represent
7 MGEs. Size of nodes and thickness of edges indicates their weight (occurrence frequency).
8 Numbers alongside shared genes are their indexes in the representative gene set, and numbers in
9 parentheses indicate loci of these genes in the reference genome.

10
11
12
13
14
15 **Supplementary Figure S2.** Examples of arrangement determined by the algorithm. (a)
16 arrangements for shared nodes (blue) and reference-specific nodes (green). (b-e) arrangements for
17 query-specific nodes (red).

18
19
20
21 **Supplementary Table S1.** Metadata of isolate genomes used in this study.

22
23
24 **Supplementary Table S2.** Statistics for the 5 mock metagenomic datasets.

25
26
27 **Supplementary Table S3.** Tables of nodes and edges in the 5-*E. coli*-genome pangenome network
28 and the 760-metagenome pangenome network.

29
30
31 **Supplementary File S1:** Texts for, 1) steps for installing the plug-in and visualizing pangenome
32 networks in Cytoscape, 2) steps for selecting query-specific nodes for arrangement, 3) Comparison
33 of the reference pangenome network (RPGN) and the query pangenome network (RPGN), 4)
34 detailed definitions of conformity and divergence for nodes and edges, and 5) supplementary
35 references.

36
37
38
39
40 **Supplementary File S2:** “5-*E. coli*-genome pangenome network.pdf”, PDF file for *E. coli*
41 pangenome network derived from five pathogenic *E.coli* strains.

42
43
44 **Supplementary File S3:** “760-metagenome pangenome network.pdf”, PDF file for *E. coli*
45 pangenome network derived from 760 genuine metagenomes.

46 47 48 49 50 51 **Abbreviations**

52
53
54 CA: colonic acid; *E. coli*: *Escherichia coli*; LPS: lipopolysaccharide; MGEs: mobile genetic
55 elements; *P. copri*: *Prevotella copri*.

Ethics approval

This study has been approved by the Institutional Review Board on Bioethics and Biosafety (reference number: BGI-IRB 16017).

Consent for publication

Not applicable.

Competing interests

The authors declare no competing interests.

Acknowledgements

This study was supported by the National Natural Science Foundation of China (No.31601073).

References

1. Tettelin H, Massignani V, Cieslewicz MJ, Donati C, Medini D, Ward NL, et al. Genome analysis of multiple pathogenic isolates of *Streptococcus agalactiae*: Implications for the microbial “pan-genome.” *Proc Natl Acad Sci [Internet]*. 2005;102:13950–5. Available from: <http://www.pnas.org/cgi/doi/10.1073/pnas.0506758102>
2. Contreras-Moreira B, Vinuesa P. GET_HOMOLOGUES, a versatile software package for scalable and robust microbial pangenome analysis. *Appl Environ Microbiol*. 2013;79:7696–701.
3. Zhao Y, Wu J, Yang J, Sun S, Xiao J, Yu J. PGAP: Pan-genomes analysis pipeline. *Bioinformatics*. 2012;28:416–8.
4. Cain AA, Kosara R, Gibas CJ. GenoSets: Visual Analytic Methods for Comparative Genomics. *PLoS One*. 2012;7.
5. Brittnacher MJ, Fong C, Hayden HS, Jacobs MA, Radey M, Rohmer L. PGAT: A multistrain analysis resource for microbial genomes. *Bioinformatics*. 2011;27:2429–30.
6. Fremez R, Faraut T, Fichant G, Gouzy J, Quentin Y. Phylogenetic exploration of bacterial genomic rearrangements. *Bioinformatics*. 2007;23:1172–4.
7. Blom J, Kreis J, Spänig S, Juhre T, Bertelli C, Ernst C, et al. EDGAR 2.0: an enhanced software platform for comparative gene content analyses. *Nucleic Acids Res*. 2016;44:W22–8.
8. Herbig A, Jäger G, Battke F, Nieselt K. GenomeRing: Alignment visualization based on SuperGenome

1
2
3
4 coordinates. *Bioinformatics*. 2012;28:7–15.
5

6 9. Pedersen TL, Nookaew I, Wayne Ussery D, Månsson M. PanViz: interactive visualization of the
7 structure of functionally annotated pangenomes. *Bioinformatics* [Internet]. 2017;33:btw761. Available
8 from: <https://academic.oup.com/bioinformatics/article-lookup/doi/10.1093/bioinformatics/btw761>
9

10 10. Marcus S, Lee H, Schatz M, Schatz MC. SplitMEM : Graphical pan-genome analysis with suffix
11 skips *BIOINFORMATICS* SplitMEM : Graphical pan-genome analysis with suffix skips. *bioArXiv*.
12 2014;0–7.
13

14 11. Baier U, Beller T, Ohlebusch E. Graphical pan-genome analysis with compressed suffix trees and the
15 Burrows-Wheeler transform. *Bioinformatics*. 2015;32:497–504.
16

17 12. Scholz M, Ward D V, Pasolli E, Tolio T, Zolfo M, Asnicar F, et al. Strain-level microbial
18 epidemiology and population genomics from shotgun metagenomics. *Nat Methods* [Internet]. Nature
19 Publishing Group; 2016; Available from: <http://www.nature.com/doi/10.1038/nmeth.3802>
20

21 13. Nayfach S, Rodriguez-Mueller B, Garud N, Pollard KS. An integrated metagenomics pipeline for
22 strain profiling reveals novel patterns of bacterial transmission and biogeography. *Genome Res*.
23 2016;26:1612–25.
24

25 14. Delmont TO, Eren AM. Linking pangenomes and metagenomes: the *Prochlorococcus*
26 metapangenome. *PeerJ* [Internet]. 2018;6:e4320. Available from: <https://peerj.com/articles/4320>
27

28 15. Kim Y, Koh I, Young Lim M, Chung WH, Rho M. Pan-genome analysis of *Bacillus* for microbiome
29 profiling. *Sci Rep*. 2017;7:1–9.
30

31 16. Farag IF, Youssef NH, Elshahed MS. Global distribution patterns and pangenomic diversity of the
32 candidate phylum “Latescibacteria” (WS3). *Appl Environ Microbiol*. 2017;83:1–21.
33

34 17. Cytoscape: An Open Source Platform for Complex Network Analysis and Visualization [Internet].
35 [cited 2017 Nov 8]. Available from: <http://www.cytoscape.org/>
36

37 18. Meredith TC, Mamat U, Kaczynski Z, Lindner B, Holst O, Woodard RW. Modification of
38 lipopolysaccharide with colanic acid (M-antigen) repeats in *Escherichia coli*. *J Biol Chem*.
39 2007;282:7790–8.
40

41 19. Guy L, Jernberg C, Arvén Norling J, Ivarsson S, Hedenström I, Melefors Ö, et al. Adaptive Mutations
42 and Replacements of Virulence Traits in the *Escherichia coli* O104:H4 Outbreak Population. *PLoS One*.
43 2013;8.
44

45 20. Rasko DA, Webster DR, Sahl JW, Bashir A, Boisen N, Scheutz F, et al. Origins of the *E. coli* Strain
46 Causing an Outbreak of Hemolytic–Uremic Syndrome in Germany. *N Engl J Med* [Internet].
47 2011;365:709–17. Available from: <http://www.nejm.org/doi/abs/10.1056/NEJMoa1106920>
48

49 21. Qin J, Li R, Raes J, Arumugam M, Burgdorf KS, Manichanh C, et al. A human gut microbial gene
50 catalogue established by metagenomic sequencing. *Nature*. Macmillan Publishers Limited. All rights
51 reserved; 2010;464:59–65.
52

53 22. Le Chatelier E, Nielsen T, Qin J, Prifti E, Hildebrand F, Falony G, et al. Richness of human gut
54 microbiome correlates with metabolic markers. *Nature*. 2013;500:541–6.
55

56 23. Nielsen HB. Identification and assembly of genomes and genetic elements in complex metagenomic
57 samples without using reference genomes. *nbt*. 2014;2014:41–5.
58

59 24. Li J, Jia H, Cai X, Zhong H, Feng Q, Sunagawa S, et al. An integrated catalog of reference genes in
60 the human gut microbiome. *Nat Biotech* [Internet]. 2014;advance on:834–41. Available from:
61
62
63
64
65

- 1
2
3
4 <http://dx.doi.org/10.1038/nbt.2942>[http://www.nature.com/nbt/journal/vaop/ncurrent/abs/nbt.2942.html#supplementary-](http://www.nature.com/nbt/journal/vaop/ncurrent/abs/nbt.2942.html#supplementary-information)
5 [information](http://www.nature.com/nbt/journal/v32/n8/full/nbt.2942.html?WT.ec_id=NBT-201408)
6 [http://www.nature.com/nbt/journal/v32/n8/full/nbt.2942.html?WT.ec_id=NBT-](http://www.nature.com/nbt/journal/v32/n8/full/nbt.2942.html?WT.ec_id=NBT-201408)
7 [201408](http://www.ncbi.nlm.nih.gov)
8 <http://www.ncbi.nlm.nih.gov>
9
10 25. Darmon E, Leach DRF. Bacterial Genome Instability. *Microbiol Mol Biol Rev* [Internet]. 2014;78:1–
11 39. Available from: <http://mmbbr.asm.org/cgi/doi/10.1128/MMBR.00035-13>
12
13 26. Whitfield C, Valvano M a. Species-Wide Variation in the Escherichia coli Flagellin. *Adv Microb*
14 *Physiol.* 2003;35:135–246.
15
16 27. Reid SD, Selander RK, Whittam TS. Sequence diversity of flagellin (fliC) alleles in pathogenic
17 *Escherichia coli*. *J Bacteriol.* 1999;181:153–60.
18
19 28. Beutin L, Delannoy S, Fach P. Sequence variations in the flagellar antigen genes *fliC*
20 and *fliC* of *Escherichia coli* and their use in identification and characterization of
21 enterohemorrhagic *E. Coli* (EHEC) O145:H25 and O145:H28. *PLoS One.* 2015;10.
22
23 29. Heinrichs DE, Yethon JA, Whitfield C. Molecular basis for structural diversity in the core regions of
24 the lipopolysaccharides of *Escherichia coli* and *Salmonella enterica*. *Mol. Microbiol.* 1998. p. 221–32.
25
26 30. Iguchi A, Iyoda S, Kikuchi T, Ogura Y, Katsura K, Ohnishi M, et al. A complete view of the genetic
27 diversity of the *Escherichia coli* O-antigen biosynthesis gene cluster. *DNA Res.* 2015;22:101–7.
28
29 31. Huynen M, Snel B, Lathe W, Bork P. Predicting protein function by genomic context: Quantitative
30 evaluation and qualitative inferences. *Genome Res.* 2000;10:1204–10.
31
32 32. Delihans N. Impact of small repeat sequences on bacterial genome evolution. *Genome Biol Evol.*
33 2011;3:959–73.
34
35 33. Wang D, Li S, Guo F, Ning K, Wang L. Core-genome scaffold comparison reveals the prevalence that
36 inversion events are associated with pairs of inverted repeats. *BMC Genomics* [Internet]. *BMC*
37 *Genomics*; 2017;18:268. Available from:
38 <http://bmcbgenomics.biomedcentral.com/articles/10.1186/s12864-017-3655-0>
39
40 34. Doron S, Melamed S, Ofir G, Leavitt A, Lopatina A, Keren M, et al. Systematic discovery of
41 antiphage defense systems in the microbial pangenome. *Science* (80-). 2018;1–17.
42
43 35. Serruto D, Serino L, Massignani V, Pizza M. Genome-based approaches to develop vaccines against
44 bacterial pathogens. *Vaccine.* 2009. p. 3245–50.
45
46 36. Maione D, Margarit I, Rinaudo CD, Massignani V, Scarselli M, Tettelin H, et al. Identification of a
47 Universal Group B Streptococcus Vaccine by Multiple Genome Screen. 2006;309:148–50.
48
49 37. Kovatcheva-Datchary P, Nilsson A, Akrami R, Lee YS, De Vadder F, Arora T, et al. Dietary Fiber-
50 Induced Improvement in Glucose Metabolism Is Associated with Increased Abundance of *Prevotella*. *Cell*
51 *Metab.* 2015;22:971–82.
52
53 38. Pedersen HK, Gudmundsdottir V, Nielsen HB, Hyotylainen T, Nielsen T, Jensen BAH, et al. Human
54 gut microbes impact host serum metabolome and insulin sensitivity. *Nature.* 2016;535:376–81.
55
56 39. Laursen BS, Sørensen HP, Mortensen KK, Sperling-Petersen HU. Initiation of protein synthesis in
57 bacteria. *Microbiol Mol Biol Rev* [Internet]. 2005;69:101–23. Available from:
58 <http://www.scopus.com/inward/record.url?eid=2-s2.0-14844340954&partnerID=tZOtx3y1>
59
60 40. De Boer HA, Hui AS. Sequences within ribosome binding site affecting messenger RNA
61 translatability and method to direct ribosomes to single messenger RNA species. *Methods Enzymol.*
62
63
64
65

1
2
3
4 1990;185:103–14.
5

6 41. Berwal SK, Sreejith RK, Pal JK. Distance between RBS and AUG plays an important role in
7 overexpression of recombinant proteins. *Anal Biochem.* 2010;405:275–7.
8

9 42. Zhu W, Lomsadze A, Borodovsky M. Ab initio gene identification in metagenomic sequences.
10 *Nucleic Acids Res.* 2010;38.
11

12 43. Li W, Godzik A. Cd-hit: A fast program for clustering and comparing large sets of protein or
13 nucleotide sequences. *Bioinformatics.* 2006;22:1658–9.
14

15 44. Kent WJ. BLAT - The BLAST-like alignment tool. *Genome Res.* 2002;12:656–64.
16

17 45. Mende DR, Waller AS, Sunagawa S, Järvelin AI, Chan MM, Arumugam M, et al. Assessment of
18 metagenomic assembly using simulated next generation sequencing data. *PLoS One.* 2012;7.
19

20 46. R: The R Project for Statistical Computing [Internet]. [cited 2018 Mar 6]. Available from:
21 <https://www.r-project.org/>
22
23
24
25
26
27
28
29
30
31
32
33
34
35
36
37
38
39
40
41
42
43
44
45
46
47
48
49
50
51
52
53
54
55
56
57
58
59
60
61
62
63
64
65

Table 1. Comparison of several pangenome analysis methods.

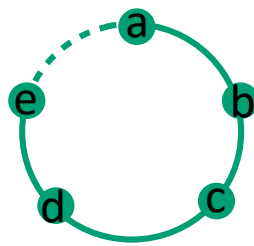
Method	Input	
	Isolate genomes	Metagenomes
GET_HOMOLOGUES [2] and PGAP [3]	Yes	No
GenoSets [4], PGAT [5], PEGR [6], EDGAR [7], GenomeRing [8]	Yes	No
PanViz [9]	Yes	No
SplitMEM10 and a tool introduced by Baier <i>et al.</i> [11]	Yes	No
PanPhlAn [12], MIDAS [13] and a method introduced by Farag <i>et al.</i> [16]	No	Yes
MetaPGN	Yes	Yes

Output			Functionality	
Gene content	Gene-gene adjacency	Network	Biological annotation	Interactive visualization
Yes	No	No	Yes	No
Yes	Yes	No	Yes	No
Yes	Yes	No	Yes	Yes
Yes	Yes	Yes	No	Yes
Yes	No	No	Yes	No
Yes	Yes	Yes	Yes	Yes

Figure 1

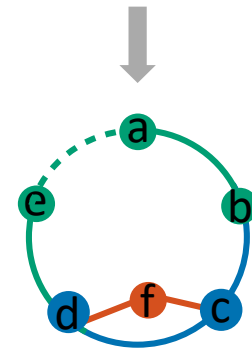
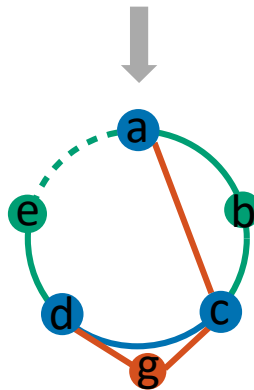
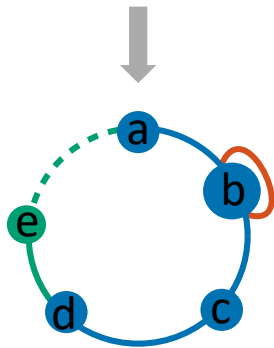
[Click here to download Figure Figure 1.pdf](#)

Reference genome

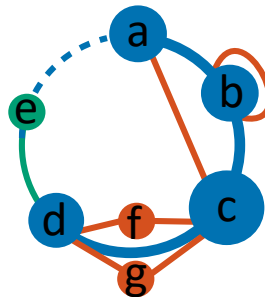


+

Query assemblies



Pangenome network



Node/Edge

- █ reference-specific
- █ shared
- █ query-specific

Node

Name	Freq.	From	Gene	Annotation	...
a	3	S1, S2, Ref	<i>fliA</i>	Sigma factor 28	...
b	2	S1, Ref	<i>fliD</i>	Flagellar capping protein	...
c	4	S1, S2, S3, Ref	<i>fliC</i>	Flagellin	...
d	4	S1, S2, S3, Ref	<i>fliZ</i>	Flagellar assembly chaperone	...
e	1	Ref	Unknown	Unknown	...
...

Edge

Source	Target	Freq.	From	...
a	b	2	S1, Ref	...
b	c	2	S1, Ref	...
b	b	1	S1	...
c	d	2	S1, Ref	...
a	c	1	S2	...
...	...			

Figure 2

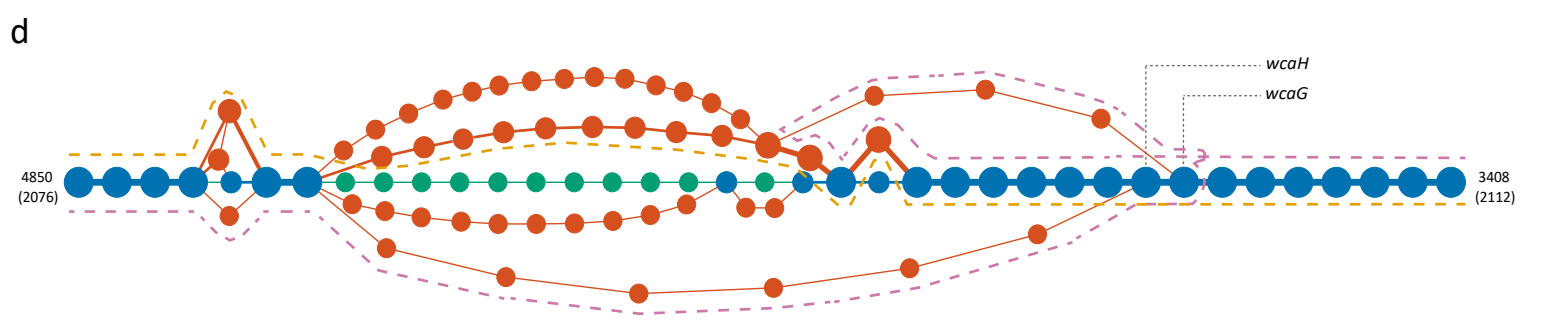
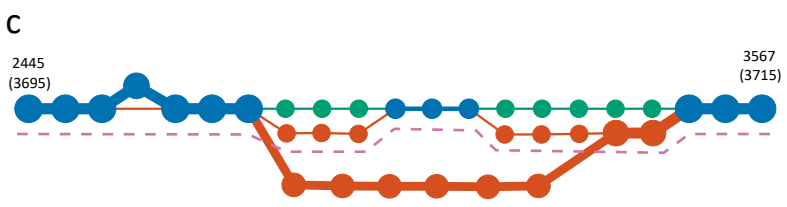
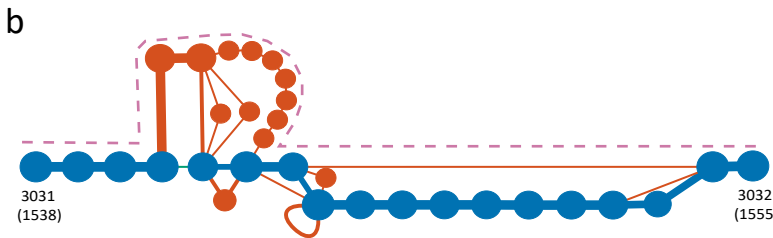
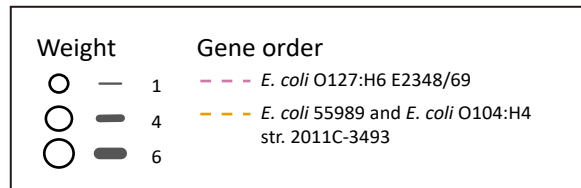
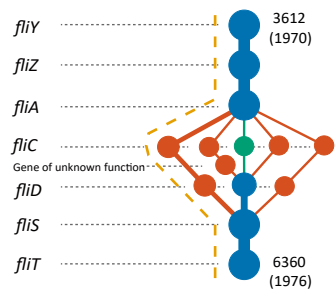
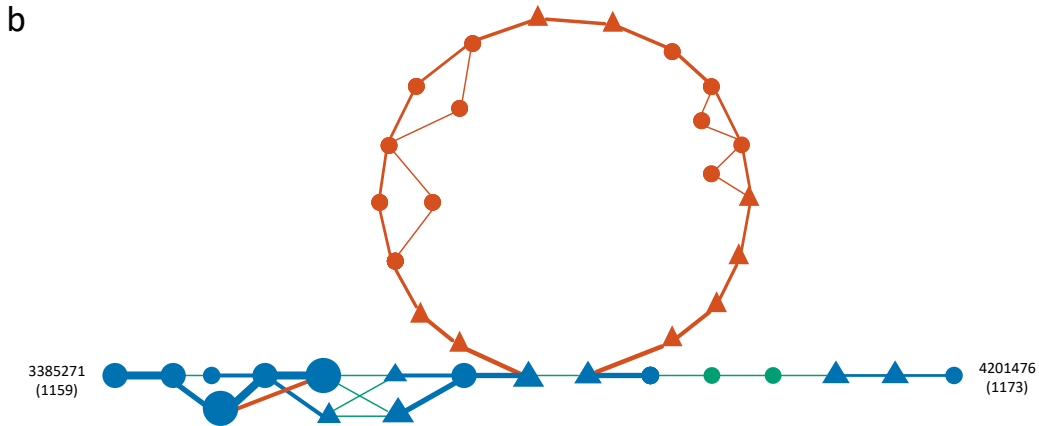
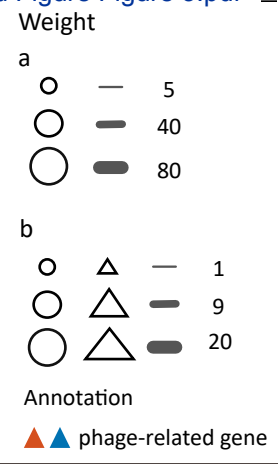
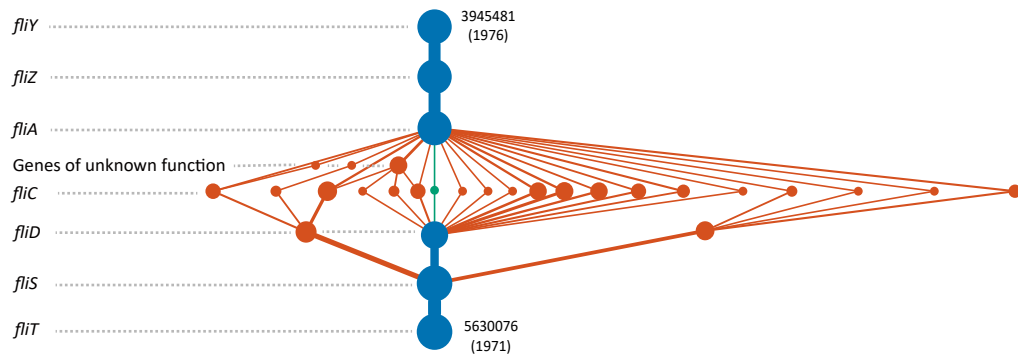
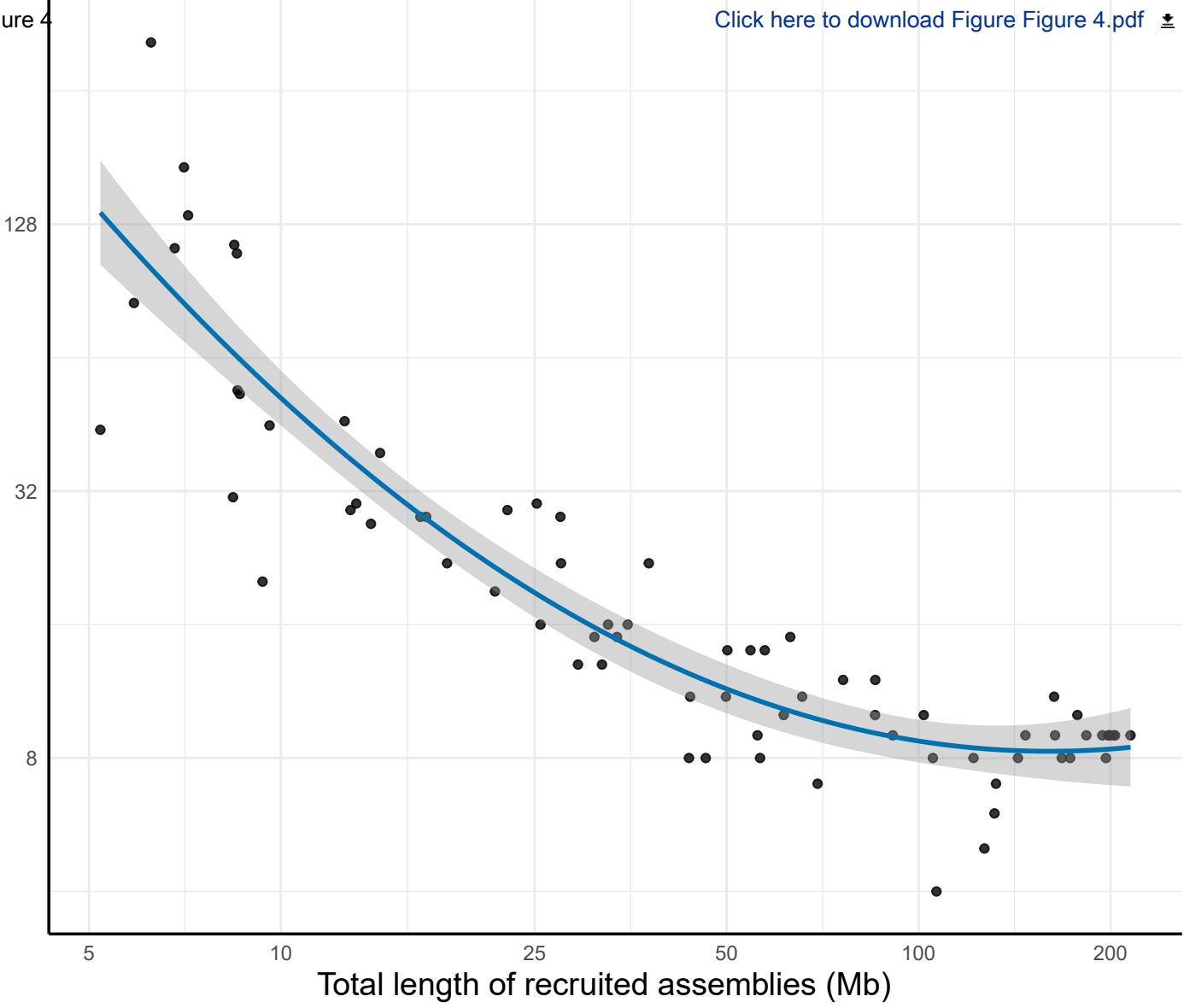


Figure 3

[Click here to download Figure Figure 3.pdf](#)

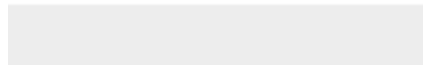


Number of subnetworks





Click here to access/download
Supplementary Material
Supplementary Figure S1.pdf





Click here to access/download
Supplementary Material
Supplementary Figure S2.pdf





Click here to access/download
Supplementary Material
Supplementary Table S1.xlsx





Click here to access/download
Supplementary Material
Supplementary Table S2.xlsx



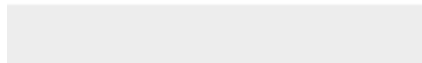


Click here to access/download
Supplementary Material
Supplementary Table S3.xlsx



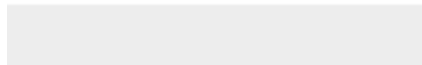


Click here to access/download
Supplementary Material
Supplementary File S1.docx





Click here to access/download
Supplementary Material
Supplementary File S2.pdf





Click here to access/download
Supplementary Material
Supplementary File S3.pdf

